0 0 0 0 4 2 0 1 1 3 6

Submitted to Chemical Physics Letters

LBL-3158
Preprint c.1

ELASTIC DIFFERENTIAL CROSS SECTIONS AND INTERMOLECULAR POTENTIALS FOR Ar + CH_4 AND Ar + NH_3

Richard Behrens, Jr., Andrew Freedman, Ronald R. Herm, and Timothy P. Parr

July 1975

Prepared for the U. S. Energy Research and Development Administration under Contract W-7405-ENG-48

For Reference

Not to be taken from this room

LAWRENCE BERKELEY LABORATORY
UNIVERSITY OF CALIFORNIA
BERKELEY

LBL-3158
c.1

DISCLAIMER

This document was prepared as an account of work sponsored by the United States Government. While this document is believed to contain correct information, neither the United States Government nor any agency thereof, nor the Regents of the University of California, nor any of their employees, makes any warranty, express or implied, or assumes any legal responsibility for the accuracy, completeness, or usefulness of any information, apparatus, product, or process disclosed, or represents that its use would not infringe privately owned rights. Reference herein to any specific commercial product, process, or service by its trade name, trademark, manufacturer, or otherwise, does not necessarily constitute or imply its endorsement, recommendation, or favoring by the United States Government or any agency thereof, or the Regents of the University of California. The views and opinions of authors expressed herein do not necessarily state or reflect those of the United States Government or any agency thereof or the Regents of the University of California.

0 0 0 0 4 2 0 1 1 5 7

ELASTIC DIFFERENTIAL CROSS SECTIONS AND INTERMOLECULAR POTENTIALS FOR Ar + CH_4 AND Ar + NH_3

Richard Behrens, Jr., Andrew Freedman,
Ronald R. Herm, and Timothy P. Parr

Inorganic Materials Research Division, Lawrence Berkeley Laboratory
and Department of Chemistry, University of California, Berkeley
and
Ames Laboratory-ERDA and Department of Chemistry
Iowa State University, Ames, Iowa 50010*

ABSTRACT

Differential elastic cross sections are reported for CH_4 + Ar ($E = \mu g^2/2 = 8.43$ kJ/mole) and NH_3 + Ar ($E = 8.31$ kJ/mole) in the region of the rainbow angles. Quantum interference undulations are observed as well for CH_4 + Ar and, possibly, NH_3 + Ar. The measurements are fit to spherically symmetric intermolecular potentials yielding well depths and equilibrium intermolecular separations of 1.32 kJ/mole and 3.82 Å for CH_4 + Ar and 1.32 kJ/mole and 3.92 Å for NH_3+ Ar.

* Present address.

Intermolecular potentials in the alkali + rare gas and rare gas + rare gas systems have now been determined from high resolution measurements of the elastic differential cross section. The validity of interpreting similar measurements on atom + molecule and molecule + molecule systems in terms of a spherically symmetric intermolecular potential remains unclear however. The extent to which features of the elastic cross section are broadened, shifted, or quenched by anisotropic interaction terms and possible inelastic transitions can be ascertained only by examining a wide variety of collision partners. The CH_4, NH_3, H_2O, HF sequence is especially suited for such study because of the systematic symmetry changes. Moreover, the relatively large rotation constants in these hydrides might permit complementary high resolution studies of their inelastic scattering. This paper represents an initial attack on this problem and reports high resolution differential cross sections for elastic scattering of CH_4 and NH_3 from Ar.

APPARATUS AND EXPERIMENTAL PROCEDURE

The ability to observe fine structure in elastic scattering measurements is very dependent on the angular and beam speed resolutions of the crossed beam apparatus. Although described in detail in Ref. 1, the apparatus[2] has not been described previously in the open literature. Figure 1 illustrates that stainless steel gas reservoirs (14) which are housed in vacuum chambers (6 and 7) pumped by 10" diffusion pumps

serve as two nozzle beam sources. These nozzle beams traverse skimmers (13), collimating vacuum chambers (4 and 5), and collimating slits (11 and 12) to intersect at 90° in the main vacuum chamber (22). The detector assembly, which is housed in differentially pumped chambers 1, 2, and 3, may be rotated about the beam intersection region (BIR). Chambers 1 and 2 are each equipped with ion and Ti- sublimator pumps; chamber 3 is equipped with ion and liquid He pumps. The detector's ability to view the BIR is limited by square orifices on the entrances to chamber 1 (item 8 : 0.38 cm wide, 4.4 cm from BIR) and the ionizer (item 10:0.30 cm. wide, 18.4 cm from BIR). Item 8 is actually mounted on a gate valve which permits vacuum isolation of chambers 1, 2, and 3 when experiments are not in progress. The detector consists of a Brink type ionizer in chamber 3 followed by an EAI -Quad 250 mass-filter and scintillation counter in chamber 2.

Modifications on the basic design described in Ref. 3 included the following: (a) A nickel-plated copper chamber (LN_2 cooled; not shown in Fig. 1) is actually enclosed within the walls of chamber 22. The space between these two chambers is pumped separately and serves as a beam trap by means of holes in the copper chamber and associated wedges on item 22 opposite each beam which deflect molecules into this pump-out region. (b) The physical size of the vacuum chamber has been increased to accommodate an 89 cm diameter rotatable seal for the detector assember in order to improve the angular and time-of-flight (item 20 for inelastic or reactive scattering studies) resolution of the detector. This also increased conductances to the pumps of chambers 1, 2 and 3. (c) The detector assembly chamber walls (21)

are cooled by LN_2. In conjunction with (b), this results in typical background pressures during an experiment of $\sim 3 \times 10^{-9}$ Torr in chamber 1 and $\sim 3 \times 10^{-10}$ Torr in chambers 2 and 3. (d) The movable gate valve (8) is also equipped with a 0.075 cm diameter circular orifice which is used when measuring angular or speed distributions of an intense nozzle beam.

Table I lists nozzle beam conditions. Neither beam was of sufficient intensity to measurably attenuate ($\sim$0.5%) the other beam. The Ar beam was modulated at $\sim$ 55 Hz by a rotating wheel (18) and the modulated CH_4 or NH_3 scattered signal was detected. The scattered angular distribution was measured two or three times during an apparatus pump-down; data for CH_4 + Ar is the average of two pump-downs. Reference angle readings were collected as every third to fifth data point to correct for long-term drifts in apparatus sensitivity. Counting times were 40 seconds for data below 10°, and 80 or 120 seconds at wider angles. Error bars shown are the larger of standard deviations based on the absolute counts collected for one point or the result of averaging two or more points. As a check against possible systematic errors, the Ar + O_2 elastic differential cross section was measured in the vicinity of the rainbow angle; this data was well-fit[1] by the potential parameters reported in Ref. 4.

RESULTS AND DATA ANALYSIS

The rainbow structure is quite apparent in the data shown in Fig. 2 where the measured laboratory (LAB) angular distribution, $N_L(\Theta)$, has been multiplied by the $\Theta^{4/3} \sin \Theta$ small angle scattering form-factor. The data analysis procedure[5] described in Ref. 6 was followed. Briefly, this consists in assuming a form for the spherically symmetric intermolecular potential, V(r), calculating the phase shifts, $\eta_\ell(g)$, for each

partial wave quantum number as a function of relative collision speed, g, by means of the JWKB approximation, and finally summing the contributions of each partial wave to obtain the scattering amplitude, $f(\theta, g)$, as a function of center-of-mass (CM) scattering angle, θ. A predicted LAB angular distribution, $N_p(\Theta)$, is calculated from $f(\theta, g)$ by averaging the CM→LAB transformation over beam speed distributions and detector angular resolution. The angular resolution variables introduced in Ref. 6(Eq. (3)) were $X_0 = 0.47°$ and X_1 = half-angle subtended by the (Θ-dependent) BIR at the ionizer entrance slit. Potential parameters are varied so as to obtain the best fit to the data of Fig. 2 by minimizing χ^2(Eq. (5) of Ref. 6).

The MSV potential introduced in Ref. 6 provides a convenient, flexible representation which is given in reduced units in terms of the well depth ϵ and its position r_m by

$$\varphi(x) = V(r/r_m)/\epsilon,$$

$$\varphi_I(x) = \exp[-2\beta(x-1)] - 2\exp[-\beta(x-1)], \qquad x \leq x_3 \qquad (1)$$

$$\varphi_{II}(x) = b_1 + (x-x_3)\left\{b_2 + (x-x_4)[b_3 + (x-x_3)b_4]\right\}, \quad x_3 < x < x_4$$

$$\varphi_{III}(x) = -c_6 x^{-6} \qquad x_4 \leq x$$

where $c_6 = C_6/\epsilon r_m^6$ is the van der Waals dispersion constant in reduced units. The role of φ_{II} is to connect φ_I and φ_{III} smoothly by adjusting the b coeffieients to make $\varphi(x)$ and $\varphi'(x)$ continuous at x_3 and x_4. Following the procedure of Ref. 6, x_4 was set equal to 1.4 and x_3 was fixed by requiring $\varphi(x_3) = -0.75$ with $\varphi'(x_3) > 0$. Since the C_6 values are taken from the literature, only ϵ, r_m, and β remain as adjustable parameters. For CH_4+ Ar, C_6 was taken from Ref. 7. For NH_3+ Ar, the dispersion constant for NH_3+ NH_3 was first estimated from the Slater-Kirkwood approximation[7] using the NH_3 polarizability recommended by Hirschfelder[8];

C_6 for NH_3+ Ar was then obtained by adding the relatively small angle-averaged dipole-induced dipole contribution to the dispersion constant obtained from the Kramer-Herschbach formula (Eq. (1) of Ref. 7).

Parameters of the MSV potential which provided the best fit to the data are listed in Table II. The χ^2 entries indicate that the fit was appreciably better for the CH_4 + Ar data. The limit on ϵ, r_m, and β indicate the change of any one variable, holding the others constant, required to produce a significant deterioration in the fit; this range corresponded to an increase in χ^2 to 2.5 for CH_4+ Ar and 3.1 for NH_3+ Ar. In order to test the sensitivity of the fit to the assumed functional form, the data were also fit to a Lennard-Jones (LJ) n-6 potential:

$$\varphi(x) = [n/(n-6)]\,[(6/n)x^{-n} - x^{-6}]\,. \qquad (2)$$

Since it was constrained to the proper c_6/x^6 asymptotic behavior, this potential provided only two adjustable parameters. Nevertheless, an equally good fit to the CH_4+ Ar data was obtained for ϵ = 1.37 kJ/mole and r_m = 3.77 Å in an L-J 18-6 potential. Plots of the MSV and L-J potentials for CH_4+ Ar show them to be remarkably similar except for some inconsequential differences in the $\varphi(x) < -0.5$ region. No satisfactory fit to the NH_3+ Ar data was achieved for an L-J potential constrained to the proper asymptotic behavior.

DISCUSSION

Brooks and Grosser[9] have previously reported an elastic differential cross section for NH_3+Ar with the rainbow structure quite apparent and have fit their data to four different possible potential functions. Their reported ϵ(kJ/mole), r_m and C_6(kJ-Å^6/mole) values (C_6 calculated by us from their potentials) are: 1.40, 4.11Å, 10,000 (L-J 18-6); 1.48, 3.65 Å, 6980 (L-J 12-6); 1.35-1.40, 4.10Å, 6490(Maitland-Smith); and 1.34-1.35, 4.00-4.02Å, 4980 (Kihara-Stockmayer). Their Kihara-Stockmayer

potential comes closest to our best literature estimate of C_6 and provides ϵ and r_m values in reasonable agreement with the entries in Table II. Schimpke and Schugerl[10] have previously reported a narrow angle differential cross section for CH_4+Ar which showed the asymptotic potential dependence to be r^{-6}. However, the rainbow structure was not resolved and potential parameters were not obtained. Eckelt, Schimpke and Schugerl[11] obtained ϵ = 1.09 kJ/mole and r_m = 2.67Å by fitting their measured speed dependent CH_4+Ar total cross section to an L-J 12-6 potential, although they caution that their values may be too low. Assuming an L-J 12-6 potential, Stevens and deVries[12] obtained ϵ = 1.23 kJ/mole from their measured thermal diffusion coefficient inversion temperature for CH_4+Ar. The similarities of the CH_4 and NH_3+Ar potential parameters in Table II are striking, especially in view of the significantly different parameters for the isoelectronic Ne+Ar[13], ϵ = 0.60kJ/mole and r_m = 3.43Å.

The rapid oscillations in the data of Fig. 2 also warrant comment. Gordon, Coggliola, and Kuppermann[14] have observed diffraction structure in the differential cross section for scattering of H_2 and D_2 from a number of molecules. Data of Grosser and co-workers on Ar + NH_3[9] and D_2O[15] suggest the presence of a rapid oscillatory structure; however, these workers were unable to find a potential function which could simultaneously fit the gross structure of the rainbow and the period of these undulations. Thus, we know of no unequivocal observation for a molecule other than H_2 or D_2 of rapid oscillations in the differential cross section for elastic scattering. Indeed, there are theoretical[16] and experimental[17] indications that such features might be severely quenched by anisotropic interaction terms. Nonetheless, there are strong indications that the undulations in the CH_4+ Ar data in Fig. 2 are real. The theoretical

calculation shown in Fig. 2 indicates that the interference between larger impact parameters leading to rainbow scattering and smaller impact parameters sampling the repulsive wall of V(r) should produce ocillations in $N_L(\Theta)$ large enough to observe only on the far side of the rainbow maximum. It is noteworthy that the oscillations in the data appear only in this angular region. Moreover, the potential function derived by fitting the overall shape of the rainbow region (minimizing χ^2) reproduce the period and positions of the undulations in the data well. The limits on ϵ, r_m, and β in Table II also indicate the approximate range in these parameters which still provide a good fit to the undulations. These remarks might also apply to NH_3+ Ar (except that the limits quoted in Table II should be reduced by a factor of two to give the ranges consistent with the oscillatory structure), although the observations of undulations here is less clearly established owing to the poorer quality of the data. Observation of such interference undulations for CH_4+ Ar is consistent with the expected weak anisotropic terms for the system: the longest range anisotropic term is an r^{-7} dispersion interaction[18] and CH_4 - CH_4 thermal conductivities indicate that the repulsive CH_4 interaction should be close to spherically symmetric[19]. Persistence of these undulations in NH_3+ Ar would be more surprising but not without precedence. Rothe and Helbing[20] observed glory undulations in the total cross sections for Li + NH_3 as well as Li+ CH_4, although the amplitudes of the glory were measurably attenuated for the NH_3 system.

ACKNOWLEDGEMENTS

The equipment assembly and data collection phases of this work were supported by the USAEC through the Lawrence Berkeley Laboratory. The final interpretative phase was conducted at the Ames Laboratory and performed for the U. S. Energy Research and Development Administration under Contract No. W-7405-eng-82. We are also indebted to members of the Berkeley Chemistry Department machine shop, especially Clay Taylor, Frank Lopez, Bob Waite, Carl Baugh, and Slim Bohac, for their helpful suggestions and expert fabrication of much of this apparatus.

REFERENCES

1. R. Behrens, Jr., Ph. D. thesis, University of California, Berkeley (1975).
2. Prof. Yuan Lee kindly furnished plans of his initial University of Chicago apparatus which proved very helpful in the design of this apparatus.
3. Y. T. Lee, J. D. McDonald, P. R. LeBreton and D. R. Herschbach, Rev. Sci. Instr. 40, 1402 (1969).
4. F. P. Tully and Y. T. Lee, J. Chem. Phys. 57, 866 (1972).
5. This data analysis program was kindly furnished by Prof. Yuan Lee.
6. P. E. Siska, J. M. Parson, T. P. Schaffer and Y. T. Lee, J. Chem. Phys. 55, 5762 (1971).
7. H. L. Kramer and D. R. Herschbach, J. Chem. Phys. 53, 2792 (1970).
8. J. O. Hirschfelder, C. F. Curtiss and R. B. Bird, Molecular Theory of Gases and Liquids, John Wiley and Sons, New York, 1954.
9. R. Brooks and A. E. Grosser, Mol. Phys. 28, 593 (1974).
10. B. Schimpke and K. Schugerl, Z. Physik. Chem. Neue Folge 75, 32 (1971).
11. W. R. Eckelt, B. Schimpke and K. Schugerl, Z. Physik. Chem. Neue Folge 68, 266 (1969).
12. G. A. Stevens and A. E. deVries, Physica 39, 346 (1968).
13. C. Y. Ng, Y. T. Lee and J. A. Barker, J. Chem. Phys. 61, 1996 (1974).
14. R. J. Gordon, M. J. Coggliola and A. Kuppermann, Chem. Phys. Letters 20, 493 (1973).

15. R. Brooks, F. Kalos and A. E. Grosser, Mol. Phys. 27, 1071 (1974).

16. R. J. Cross, Jr., J. Chem. Phys. 52, 5703 (1970).

17. K. G. Anlauf, R. W. Bickes, Jr., R. B. Berstein, J. Chem. Phys. 54, 3647 (1971).

18. A. D. Buckingham, Adv. Chem. Phys. 12, 107 (1967).

19. J. D. Verlin, E. R. Cooper and D. K. Hoffman, J. Chem. Phys. 56, 3740 (1972).

20. E. W. Rothe and R. K. B. Helbing, J. Chem. Phys. 53, 2501 (1970).

Table I. Experimental nozzle conditions.[a]

	d	ℓ	s	y	w	δ	P_o	T_o	M	E
CH_4	0.010	0.0025	0.07	0.6	0.18	1.3°	760	295	8.0	
Ar	0.010	0.010	0.05	1.4	0.20	1.5°	760	295	20	8.43
NH_3	0.010	0.0025	0.07	1.0	0.08	0.6°	400	295	7.2	
Ar	0.010	0.010	0.05	1.2	0.20	1.5°	750	295	20	8.31

[a] Lengths in cm; source pressures, P_o, in Torr; source temperature, T_o, in °K; and relative collision energy, E, in kJ/moles. Other symbols refer to: d - nozzle throat diameter of length ℓ; s - skimmer orifice diameter (84° and 60° external angles for CH_4 - NH_3 and Ar respectively); y - nozzle to shimmer distance; w - beam width (FWHM) at BIR; δ - beam angular width (FWHM). Mach numbers, M, were obtained by fitting measured nozzle number density speed distributions to $v^2 \exp\left\{-[(1+(\gamma-1)M^2/2)^{1/2} v/\alpha_o - \gamma^{1/2} M/\sqrt{2}]^2\right\}$ with $\alpha_o = 2kT_o/m$ and $\gamma = C_P/C_V = 5/3$ for Ar and 4/3 for CH_4 and NH_3. The entry of M = 20 for Ar is only a lower limit.

0 0 0 0 4 2 0 1 1 6 8

Table II. Parameters of the MSV Potential (Eq. 1) which best fit the data of Fig. 2.[a]

	CH_4 + Ar	NH_3 + Ar
ϵ	1.32±0.015	1.32±0.025
r_m	3.82±0.025	3.92±0.04
β	7.05±0.35	8.45±0.7
C_6	5660	5420
x_3	1.10	1.08
x_4	1.40	1.40
b_1	-0.75	-0.75
b_2	1.89	1.89
b_3	-5.41	-7.36
b_4	5.50	1.08
χ^2	1.5	2.3

[a] r_m in Å, ϵ in kJ/mole, C_6 in kJ-Å^6/mole, other parameters dimensionless.

FIGURE CAPTIONS

Fig. 1. Cross sectional view of apparatus viewed from above. Items not discussed in text are: 9-detector chamber 2 entrance slit; 15-tube for circulating fluid to heat or cool nozzle; 16-gas inlets; 17 and 19- beam flags.

Fig. 2. Data points show measured LAB angular distribution plotted as $\Theta^{4/3} \sin \Theta N_L(\Theta)$ versus LAB scattering angle Θ for CH_4+ Ar and NH_3+Ar(CH_4 or NH_3 beam direction taken as $\Theta = 0°$). Error bars smaller than the data symbol are not shown. Solid curves show fits to the data for MSV potential parameters listed in Table II.

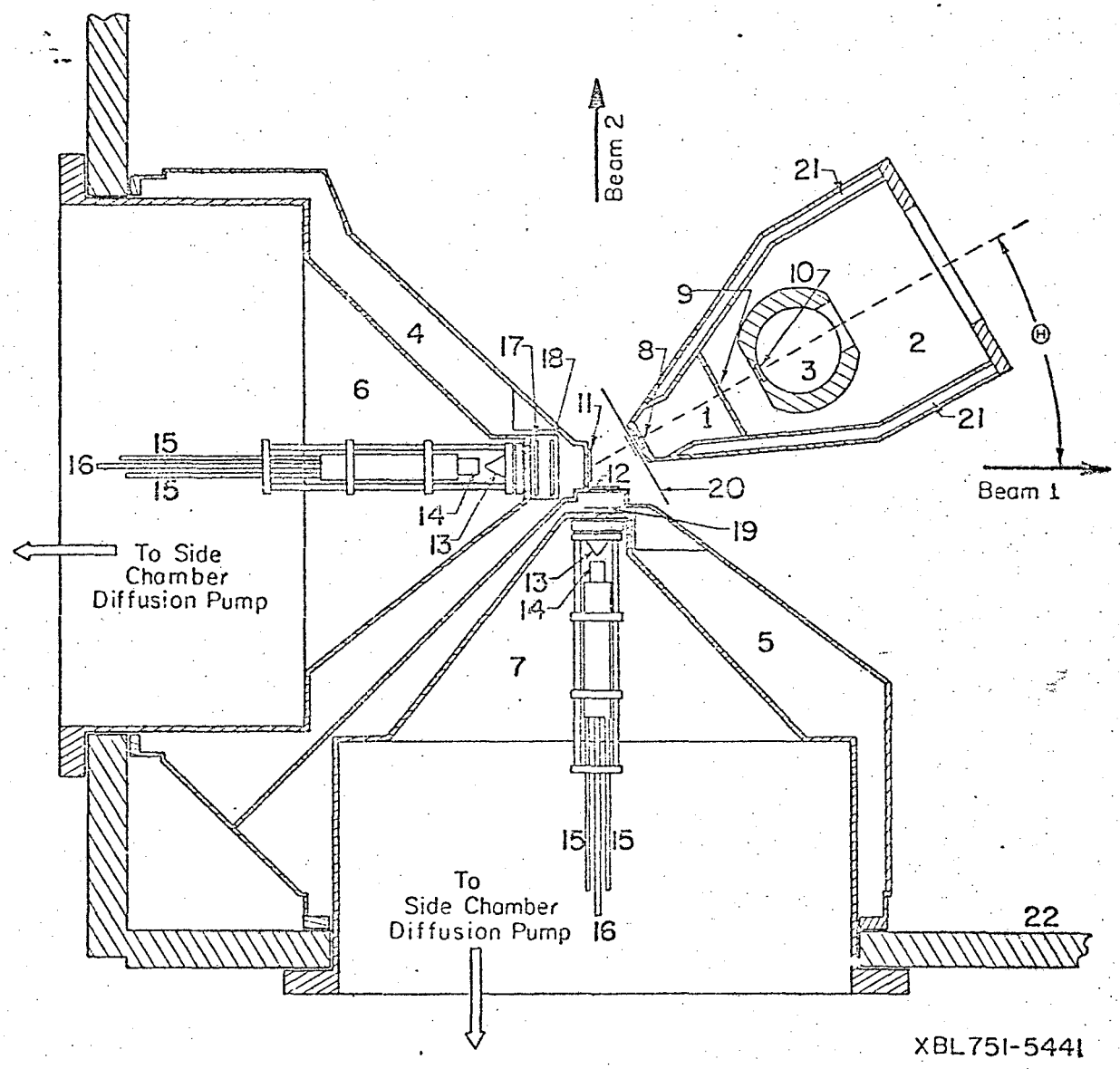
Beam 2
Beam 1
To Side Chamber Diffusion Pump
To Side Chamber Diffusion Pump
XBL751-5441

Fig. 1

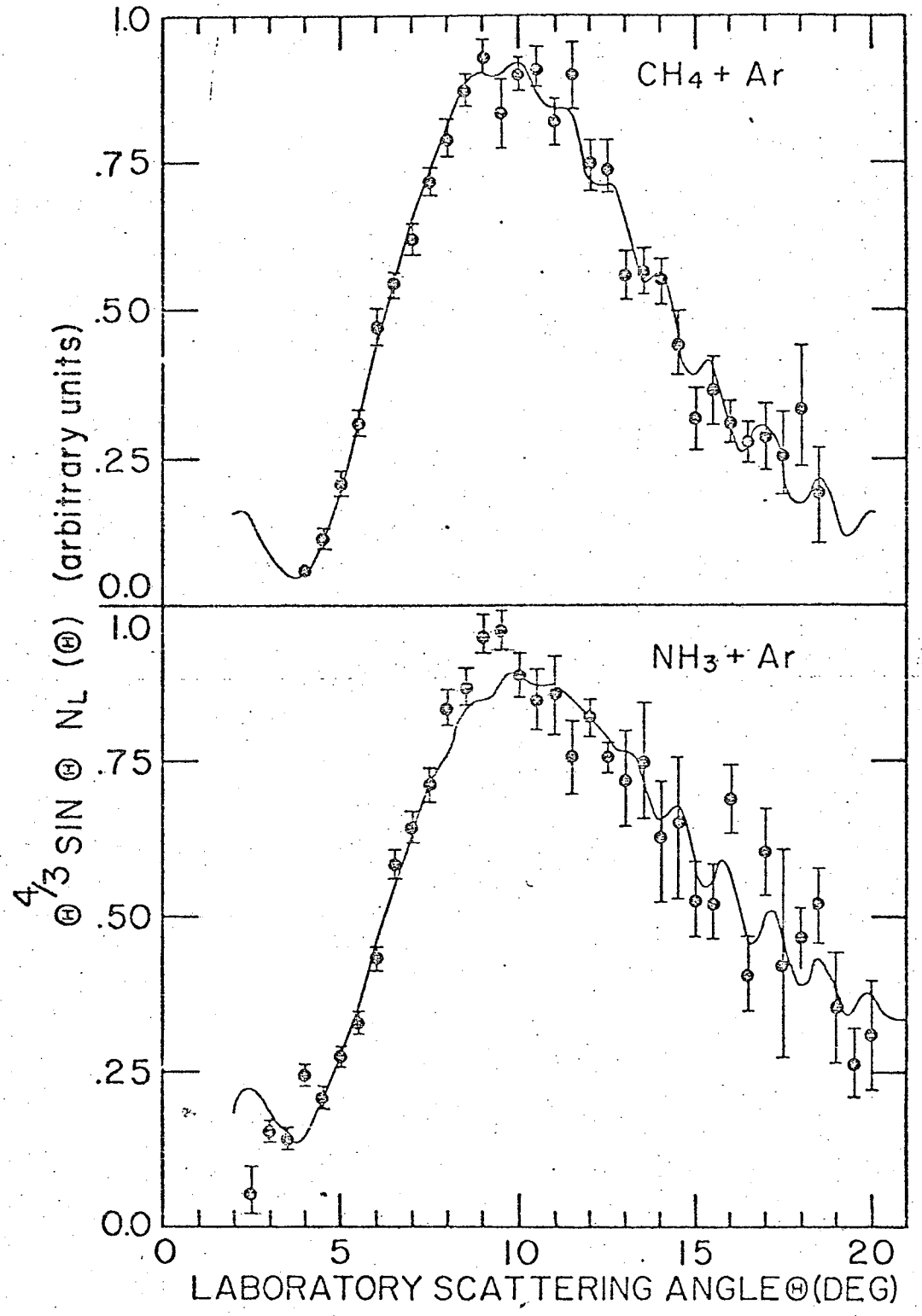
CH4 + Ar
NH3 + Ar
1.0
.75
.50
.25
0.0
4/3 SIN Θ N_L (Θ) (arbitrary units)
0
5
10
15
20
LABORATORY SCATTERING ANGLE Θ (DEG)

Fig. 2

0 0 0 0 4 2 0 1 1 7 3

LEGAL NOTICE

This report was prepared as an account of work sponsored by the United States Government. Neither the United States nor the United States Energy Research and Development Administration, nor any of their employees, nor any of their contractors, subcontractors, or their employees, makes any warranty, express or implied, or assumes any legal liability or responsibility for the accuracy, completeness or usefulness of any information, apparatus, product or process disclosed, or represents that its use would not infringe privately owned rights.

TECHNICAL INFORMATION DIVISION
LAWRENCE BERKELEY LABORATORY
UNIVERSITY OF CALIFORNIA
BERKELEY, CALIFORNIA 94720